

Article

Racemic and Meso Crystal Structures of an Axial-Chiral Spirobi-(dinaphthoazepin)ium Salt: Emergence of an S_4 -Symmetric Molecule

Philipp Honegger ^{1,*} , Natalie Gajic ², Alexander Prado-Roller ²  and Michael Widhalm ³

¹ Institute of Computational Biological Chemistry, University of Vienna, Währinger Straße 17, 1090 Vienna, Austria

² Institute of Inorganic Chemistry, University of Vienna, Währinger Straße 42, 1090 Vienna, Austria; natalie.gajic@univie.ac.at (N.G.); alexander.roller@univie.ac.at (A.P.-R.)

³ Institute of Chemical Catalysis, University of Vienna, Währinger Straße 38, 1090 Vienna, Austria; m.widhalm@univie.ac.at

* Correspondence: philipp.honegger@univie.ac.at

Abstract: To date, only a few instances of S_4 -symmetric organic molecules exist. In principle, spirobi-(dinaphthoazepin)ium cations can achieve this highly symmetric point group. Heating racemic 2,2'-bis(bromomethyl)-1,1'-binaphthyl with aqueous ammonia afforded a mixture of *rac*- and *meso*-3,3',5,5'-tetrahydro-4,4'-spirobi[dinaphtho[2,1-c:1',2'-e]azepin]-4-ium bromide which was separated by fractional crystallisation. Both stereoisomers were characterised spectroscopically, and their crystal structures were determined and compared. The *rac* crystal structure differs significantly from the known enantiopure one. The *meso* molecules display a near-perfect S_4 symmetry. Upon treatment with KO^tBu , both isomers undergo Stevens rearrangement.

Keywords: crystal structure; three-dimensional structure; chirality; axial chirality; racemate; meso; spiro compound; Stevens rearrangement



Citation: Honegger, P.; Gajic, N.; Prado-Roller, A.; Widhalm, M. Racemic and Meso Crystal Structures of an Axial-Chiral Spirobi-(dinaphthoazepin)ium Salt: Emergence of an S_4 -Symmetric Molecule. *Symmetry* **2021**, *13*, 1365. <https://doi.org/10.3390/sym13081365>

Academic Editor: Michal Rachwalski

Received: 9 July 2021

Accepted: 26 July 2021

Published: 27 July 2021

Publisher's Note: MDPI stays neutral with regard to jurisdictional claims in published maps and institutional affiliations.



Copyright: © 2021 by the authors. Licensee MDPI, Basel, Switzerland. This article is an open access article distributed under the terms and conditions of the Creative Commons Attribution (CC BY) license (<https://creativecommons.org/licenses/by/4.0/>).

1. Introduction

Dinaphthoazepinium compounds (Figure 1) have found widespread application as chiral phase transfer catalysts [1,2]. Structural variations comprised introduction of various bulky substituents (R^1 in pos. 3 and 3'), preferably using semi-rigid aromatic groups, and the quarterisation of nitrogen (R^2 = (cyclo)alkyl or benzylic moieties, etc.). Of particular interest is the formation of N-spiro compounds where a dibenzo- with a dinaphthoazepine (C) or two dinaphthoazepines (D) are merged, resulting in a conformationally stable ammonium ion [3–8]. In cases A and B, a product with C_2 symmetry is formed. The same is true for D if connecting binaphthyls with the same chirality. The situation is less obvious in case C, where the conformation of the biphenyl moiety is controlled by the binaphthyl chirality. If combining identical homochiral units in case D (R^1 = H), a spiro compound with D_2 symmetry is obtained as confirmed by X-ray analysis; from binaphthyl halves with opposite chirality, an achiral species with S_4 symmetry may result.

In view of the intended application in PTC, only non-racemic material was synthesised so far, and to the best of our knowledge, racemic precursors such as *rac*-1 have never been used as intermediate in the synthesis of 2 (Figure 2).

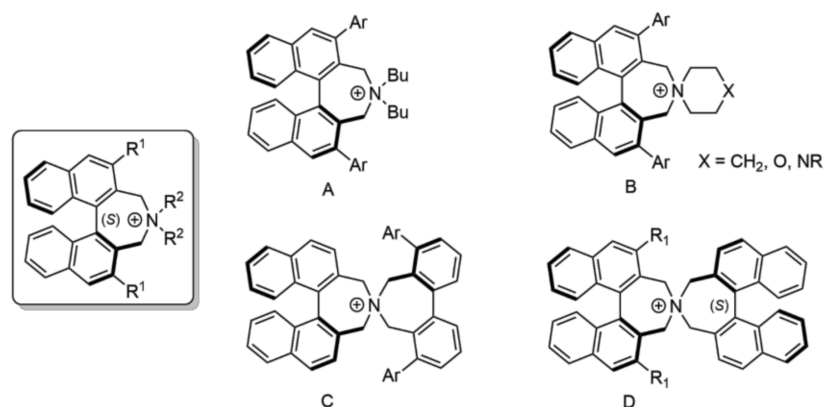


Figure 1. Dinaphthoazepinium compounds used as PTC (selection).

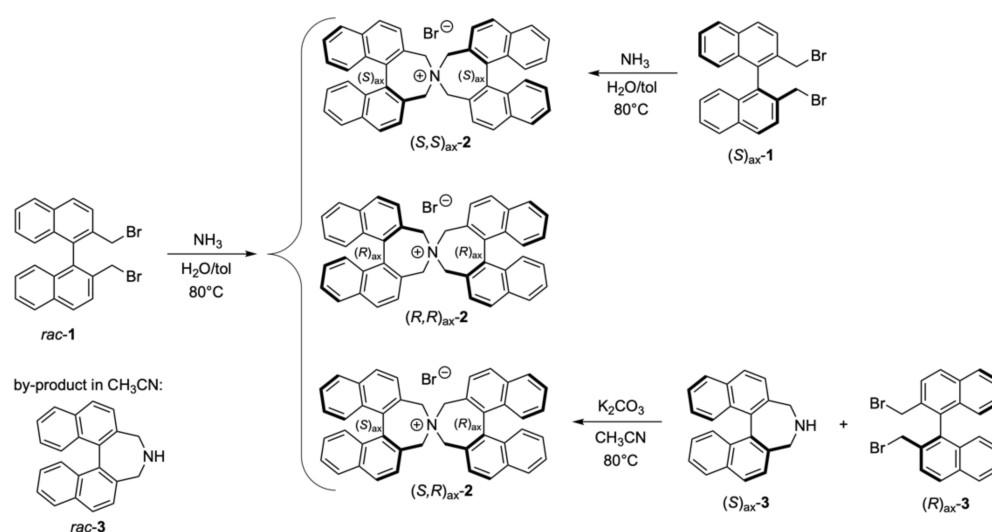


Figure 2. Synthesis of *meso*-2 and *rac*-2.

2. Materials and Methods

2.1. General

Melting points were measured on a Reichelt Thermovar Kofler apparatus, uncorrected. NMR spectra were recorded on a Bruker AV III 400 spectrometre at 400.27 MHz (^1H) and 100.66 MHz (^{13}C), and a Bruker AV III 600 at 600.25 MHz (^1H) and 150.95 MHz (^{13}C), respectively (Bruker Biospin, Billerica, MA, USA); chemical shifts δ are reported in ppm rel. to solvent signals (7.26 and 77.00 ppm for $\text{CHCl}_3/\text{CDCl}_3$, and 5.32 and 53.5 ppm for CD_2Cl_2 , respectively). Coupling patterns are designated as s(inglett), d(oublett), t(riplett), m(ultipllet), p(seudo), and br(oad). $^{13}\text{C}\{^1\text{H}\}$ NMR spectra are recorded in a J-modulated mode; signals are assigned as C, CH, CH_2 , and CH_3 . HRMS were recorded by an ESI FINNIGAN MAT 8230 mass spectrometre (Bruker Daltonics, Bremen, Germany). For HPLC determination of chiral products, an Agilent 1200 chromatograph equipped with a diode array detector and auto sampler was used (Agilent Technologies, Waldbronn, Germany).

Heptane and dichloromethane (DCM) were distilled prior to usage. Absolute THF was distilled from sodium benzophenone ketyl. All the other chemicals were analytical grade and used without further purification. Column chromatography was performed on an Isolera One system (Biotage Sweden AB, Uppsala, Sweden) with self-packed columns, SiO_2 , 40–63 μm . Racemic 2,2'-bis(bromomethyl)-1,1'-binaphthalene **1**, (*R*)_{ax}-**1**, and (*S*)_{ax}-4,5-dihydro-3H-dinaphth[2,1-c:1',2'-e]azepine (*S*)_{ax}-**3** were prepared according to literature [3,9,10].

2.2. Synthesis and Crystallisation

2.2.1. Synthesis of *meso*- and *rac*-3,3',5,5'-Tetrahydro-4,4'-spirobi[dinaphtho[2,1-c:1',2'-e]azepin]-4-ium Bromide, *meso*-2, and *rac*-2

rac-2,2'-Bis(bromomethyl)-1,1'-binaphthalene *rac*-1 (3.38 g, 7.68 mmol) was placed in a steel autoclave equipped with glass insert and stirrer. Toluene (40 mL) and aqueous ammonia (25%, 20 mL) was added, and the mixture was vigorously stirred for 24 h at 80–90 °C. After cooling to r.t., the slurry was transferred to a flask, and excess ammonia and toluene was removed under vacuum. The crystalline precipitate was separated, washed carefully with water and Et₂O, and dried to give 2.489 g (99%) of azepinium bromide **2** as mixture of *meso*-2 and *rac*-2 slightly varying in composition (45:55) separable by fractional crystallisation.

In a typical run, 1.004 g of the mixture was dissolved in THF (23 mL)/MeOH (15 mL) with gentle warming. After reducing the volume to 15 mL by slow evaporation, the crystalline material (490 mg) was separated, containing 84% of *meso*-2 and 16% of *rac*-2. A second crystallisation (20 mL THF and 10 mL MeOH) afforded 280 mg (28%) of pure *meso*-2. The mother liquor of the first crystallisation was evaporated and the residue dissolved in MeOH (4 mL). After removal of some crystalline material of low purity (148 mg), the mother liquor was evaporated to give 376 mg (37%) pure *rac*-2; mixed fractions (348 mg) could be combined and recycled.

HPLC analysis: Chiralcel-ODH (4.6 × 250 mm) in MeOH (12.5%), EtOH (12.5%), heptane (74.7%), TFA (0.3%), 0.5 mLmin⁻¹, 38 °C; t_R[(*R,S*)_{ax}-2] = 9.3 min, t_R[(*R,R*)_{ax}-2] = 11.0 min, t_R[(*S,S*)_{ax}-2] = 14.6 min (Supplementary Materials, Figure S1).

meso-2: m.p.: 315–325 °C (decomposition). ¹H NMR (CD₂Cl₂) δ: 8.15 (br.d, *J* = 8.4 Hz, 4H); 8.10 (dm, *J* = 8.2 Hz, 4H); 7.69 (d, *J* = 8.2 Hz, 4H); 7.66 (ddd, *J* = 8.1, 6.8, 1.2 Hz, 4H); 7.54 (dm, *J* = 6.8 Hz, 4H); 7.43 (ddd, *J* = 8.2, 6.9, 1.4 Hz, 4H); 4.47 (d, *J* = 12.8 Hz, 4H), 4.43 (d, *J* = 12.8 Hz, 4H) ppm.

¹³C NMR (CD₂Cl₂) δ: 137.23 (C); 134.89 (C); 131.64 (C); 130.77 (CH); 128.83 (CH); 127.84 (CH); 127.64 (CH); 127.41 (CH); 127.07 (CH); 126.23 (C); 65.17 (CH₂) ppm.

HRMS (ESI): calculated for C₄₄H₃₂N [M-Br⁺]: 574.2535, found 574.2548.

rac-2: m.p.: 330–345 °C (decomposition).

Spectroscopic data agree with literature for the non-racemic compound [3,10].

Applying the same procedure to (*R*)_{ax}-1 afforded 94% of (*R,R*)_{ax}-2.

2.2.2. Synthesis of *meso*-3,3',5,5'-Tetrahydro-4,4'-spirobi[dinaphtho[2,1-c:1',2'-e]azepin]-4-ium Bromide, (*R,S*)_{ax}-2

A mixture of (*S*)_{ax}-4,5-dihydro-3H-dinaphth[2,1-c:1',2'-e]azepine (*S*)_{ax}-3 (295 mg, 1mmol), 2,2'-bis(bromomethyl)-1,1'-binaphthalene (*R*)_{ax}-1 (440 mg, 1mmol), and K₂CO₃ (2 mmol, 280 mg) in 20 mL of acetonitrile was stirred at 80 °C for 24 h under argon. Water (50 mL) and DCM (100 mL) were added and the aqueous layer was extracted once with DCM (100 mL). The combined organic phases were dried with MgSO₄ and evaporated to give 645 mg (99%) of (*R,S*)_{ax}-2 as a pale yellow powder. ¹H NMR showed >98% purity.

2.2.3. Synthesis of 11,13,26,26a-Tetrahydrodinaphtho[2',1':3,4;1'',2'':5,6], azepino[1,2-a]dinaphtho[2,1-d:1',2'-f]azocine; (*S*)_C(*R,R*)_{ax}-4 (racemate)

To a suspension of *rac*-3,3',5,5'-tetrahydro-4,4'-spirobi[dinaphtho[2,1-c:1',2'-e]azepin]-4-ium bromide *rac*-2 (0.1 mmol) in DCM (1 mL) KO^tBu (22.5 mg, 0.2 mmol, 2 equivalents) was added. After stirring at r.t. overnight, the mixture was partitioned between water (5 mL) and DCM (5 mL). The aqueous layer was extracted with DCM (3 × 3 mL); the combined organic layers were washed with water (5 mL), dried (Na₂SO₄), and the solvent was evaporated. The residue was purified by chromatography (SiO₂, heptane/EtOAc (0–15%)) to afford 51 mg (85%) of **4** as a crystalline powder.

m.p.: 235 °C (slow decomposition above 200 °C).

^1H NMR (CDCl_3) δ : 8.01 (d, $J = 8.5$ Hz, 1H); 7.95 (d, $J = 7.0$ Hz, 1H); 7.93 (d, $J = 7.5$ Hz, 1H); 7.90 (br.d, $J = 8.5$ Hz, 2H); 7.84 (d, $J = 8.2$ Hz, 1H); 7.77 (d, $J = 8.5$ Hz, 1H); 7.76 (d, $J = 8.0$ Hz, 1H); 7.68 (d, $J = 8.5$ Hz, 1H); 7.67 (d, $J = 8.5$ Hz, 1H); 7.61 (d, $J = 8.7$ Hz, 1H); 7.41–7.50 (m, 4H); 7.40 (d, $J = 8.1$ Hz, 1H); 7.36 (m, 1H); 7.34 (m, 1H); 7.23–7.26 (m, 3H); 7.15–7.18 (m, 2H); 7.15 (d, $J = 8.5$ Hz, 1H); 4.06 (d, $J = 13.1$ Hz, 1H); 3.92 (d, $J = 14.2$ Hz, 1H); 3.85 (d, $J = 14.2$ Hz, 1H); 3.59 (m, 1H); 3.28 (d, $J = 13.1$ Hz, 1H); 3.11 (m, 2H) ppm.

^{13}C NMR (CDCl_3) δ : 140.05 (C); 138.96 (C); 138.16 (C); 135.26 (C); 133.88 (C); 133.22 (C); 133.05 (2C); 132.95 (C); 132.71 (C); 132.52 (C); 132.30 (C); 132.15 (C); 131.98 (C); 131.28 (C); 130.78 (C); 129.13 (CH); 128.96 (CH); 128.78 (CH); 128.73 (CH); 128.70 (CH); 128.38 (CH); 128.32 (CH); 128.25 (CH); 128.05 (CH); 127.80 (CH); 127.70 (3CH); 127.40 (CH); 126.41 (CH); 125.90 (CH); 125.87 (CH); 125.82 (CH); 125.69 (CH); 125.47 (CH); 125.33 (CH); 125.30 (CH); 125.02 (CH); 123.81 (CH); 63.35 (CH_2); 62.91 (CH); 60.20 (CH_2); 39.01 (CH_2) ppm.

2.2.4. Stevens Rearrangement of *meso*-2

Similar treatment of *meso*-3,3',5,5'-Tetrahydro-4,4'-spirobi[dinaphtho[2,1-c:1',2'-e]azepin]-4-ium bromide *meso*-2 as described for *rac*-2 afforded a crude mixture of rearranged products which was partly separable by MPLC (SiO_2 , heptane/EtOAc (0–10%)) to give 64% of **5** and **6** (70:30, 90% purity).

5: ^1H NMR (400 MHz, CDCl_3) δ : 6.82–8.05 (m's, 24H); 4.02 (m, 1H); 4.00 (d, $J = 10.4$ Hz, 1H); 3.99 (d, $J = 13.9$ Hz, 1H); 3.42 (dd, $J = 14.7, 5.5$ Hz, 1H); 3.30 (d, $J = 13.9$ Hz, 1H); 3.10 (dd, $J = 14.7, 3.2$ Hz, 1H); 2.99 (d, $J = 10.3$ Hz, 1H) ppm.

^{13}C NMR (151 MHz, CDCl_3) δ : 138.81 (C); 137.09 (C); 135.97 (C); 135.79 (C); 135.25 (C); 135.17 (C); 134.85 (C); 133.65 (C); 133.21 (C); 132.83 (C); 132.78 (C); 132.62 (C); 132.47 (C); 132.39 (CH); 132.30 (C); 131.30 (C); 131.07 (C); 129.29 (CH); 128.58 (CH); 128.40 (CH); 128.33 (CH); 128.02 (CH); 127.96 (CH); 127.95 (CH); 127.92 (CH); 127.89 (CH); 127.72 (CH); 127.69 (CH); 127.56 (CH); 127.44 (CH); 127.00 (CH); 126.15 (CH); 125.94 (CH); 125.76 (CH); 125.70 (CH); 125.60 (CH); 125.44 (CH); 125.38 (CH); 125.34 (CH); 125.12 (CH); 60.16 (CH_2); 54.31 (CH); 53.11 (CH_2); 38.12 (CH_2) ppm.

6: ^1H NMR (400 MHz, CDCl_3) δ : 6.73–5.15 (m's, 24H); 4.37 (d, $J = 14.2$ Hz, 1H); 4.24 (d, $J = 14.2$ Hz, 1H); 4.23 (d, $J = 8.3$ Hz, 1H); 4.06 (d, $J = 14.2$ Hz, 1H); 3.77 (d, $J = 14.2$ Hz, 1H); 2.30 (d, $J = 13.6$ Hz, 1H); 1.69 (dd, $J = 13.6, 8.3$ Hz, 1H) ppm.

^{13}C NMR (151 MHz, CDCl_3) δ : 140.95 (C); 140.74 (C); 137.19 (C); 136.18 (C); 134.77 (C); 133.62 (C); 133.12 (C); 132.78 (C); 132.62 (C); 131.89 (C); 131.65 (C); 131.61 (C); 129.90 (CH); 129.14 (CH); 128.99 (CH); 128.21 (CH); 128.11 (CH); 128.07 (CH); 127.89 (CH); 127.83 (CH); 127.64 (CH); 127.51 (CH); 127.46 (CH); 127.17 (CH); 126.97 (CH); 126.95 (CH); 125.84 (CH); 125.78 (CH); 125.60 (CH); 125.48 (CH); 125.28 (CH); 124.96 (CH); 124.72 (CH); 70.58 (CH); 58.61 (CH_2); 51.94 (CH_2); 40.13 (CH_2) ppm.

7: (95% purity); 16%. ^1H NMR (400 MHz, CDCl_3) δ : 8.00 (d, $J = 8.3$ Hz, 1H); 7.97 (dm, $J = 8.2$ Hz, 1H); 7.85–7.92 (m, 7H); 7.69 (d, $J = 8.6$ Hz, 1H); 7.66 (d, $J = 8.6$ Hz, 1H); 7.52 (d, $J = 8.0$ Hz, 1H); 7.48 (ddd, $J = 7.9, 6.7, 1.1$ Hz, 1H); 7.42 (d, $J = 8.3$ Hz, 2H); 7.38–7.43 (m, 3H); 7.36 (dm, $J = 8.7$ Hz, 2H); 7.28 (ddd, $J = 8.4, 6.9, 1.4$ Hz, 1H); 7.24 (m, 1H); 7.20 (ddd, $J = 8.2, 6.8, 1.4$ Hz, 2H); 3.86 (dd, $J = 3.6, 2.4$ Hz, 1H); 3.75 (d, $J = 12.2$ Hz, 2H); 3.32 (dd, $J = 15.0, 2.3$ Hz, 1H); 3.04 (dd, $J = 15.9, 3.7$ Hz, 1H); 3.01 (d, $J = 12.3$ Hz, 2H) ppm.

^{13}C NMR (151 MHz, CDCl_3) δ : 138.57 (C); 135.08 (C); 134.91 (2C); 134.11 (2C); 133.90 (C); 133.37 (C); 132.86 (2C); 132.24 (C); 131.27 (C); 131.22 (2C); 130.75 (C); 130.51 (C); 128.28 (CH); 128.16 (CH); 128.13 (2CH); 128.09 (2CH); 127.93 (4CH); 127.89 (CH); 127.53 (CH); 127.49 (CH); 127.39 (2CH); 126.72 (CH); 125.55 (2CH); 125.38 (CH); 125.23 (2CH); 124.90 (CH); 124.76 (CH); 124.49 (CH); 60.69 (CH); 52.52 (2 CH_2); 35.82 (CH_2) ppm.

HRMS (ESI): calculated for $\text{C}_{44}\text{H}_{32}\text{N}$ [$\text{M}+\text{H}^+$]: 574.2535, found 574.2529.

2.2.5. N-Methylation of 4

To a solution of 11,13,26,26a-Tetrahydrodinaphtho[2',1':3,4;1'',2'':5,6], azepino[1,2-a]dinaphtho[2,1-d:1',2'-f]azocine 4 (26 mg, 0.05 mmol) in acetonitrile (0.5 mL)/DCM (1.5 mL), excess of CH₃I was added and the reaction was stirred until TLC indicated absence of substrate. Evaporation of solvents left a viscous oil of pure N-methyl ammonium iodide of 4 in quantitative yield.

¹H NMR (CDCl₃) δ: 8.85 (d, *J* = 8.6 Hz, 1H); 8.16 (d, *J* = 8.7 Hz, 1H); 8.13 (d, *J* = 8.7 Hz); 8.04 (d, *J* = 8.4 Hz, 1H); 8.02 (d, *J* = 9.0 Hz, 1H); 7.98 (d, *J* = 8.4 Hz, 1H); 7.96 (d, *J* = 8.4 Hz, 1H); 7.94 (d, *J* = 8.4 Hz, 1H); 7.73 (d, *J* = 8.1 Hz, 1H); 7.66 (d, *J* = 8.4 Hz, 1H); 7.62 (ps.t, *J* = 8.5 Hz, 1H); 7.52–7.60 (m, 4H); 7.42 (m, 2H); 7.38 (m, 2H); 7.22 (ps.t, *J* = 7.7 Hz, 1H); 7.17 (ps.t, *J* = 7.9 Hz, 1H); 7.00 (d, *J* = 8.4 Hz, 2H); 6.81 (d, *J* = 8.4 Hz, 1H); 6.56 (d, *J* = 13.4 Hz, 1H); 6.23 (d, *J* = 13.0 Hz, 1H); 4.21 (d, *J* = 8.3 Hz, 1H); 4.09 (d, *J* = 12.8 Hz, 1H); 3.78 (d, *J* = 13.4 Hz, 1H); 3.67 (d, *J* = 15.8 Hz, 1H); 3.43 (dd, *J* = 15.7, 8.4 Hz, 1H); 3.01 (s, 3H) ppm.

¹³C NMR (CDCl₃) δ: 137.72 (C); 137.39 (C); 136.53 (C); 135.94 (C); 134.40 (C); 133.96 (C); 133.94 (C); 132.31 (C); 132.29 (C); 132.15 (C); 132.07 (CH); 131.61 (C); 130.89 (CH); 130.87 (C); 130.84 (CH); 130.82 (C); 130.58 (C); 130.45 (CH); 129.42 (CH); 128.82 (CH); 128.52 (CH); 128.28 (CH); 128.03 (CH); 128.01 (CH); 127.89 (CH); 127.85 (CH); 127.65 (CH); 127.48 (CH); 127.35 (CH); 127.20 (CH); 127.15 (CH); 127.10 (CH); 127.05 (2CH); 126.81 (CH); 126.47 (C); 126.24 (CH); 125.74 (CH); 123.45 (CH); 74.64 (CH); 70.47 (CH₂); 65.33 (CH₂); 42.72 (CH₃); 32.44 (CH₂) ppm.

HRMS (ESI): calculated for C₄₅H₃₄N [M-I⁺]: 588.2686, found 588.2677.

2.3. X-ray Diffractometry

The X-ray intensity data were measured on Bruker D8 Venture diffractometer equipped with multilayer monochromator, Mo K/α INCOATEC micro-focus sealed tube, and Oxford cooling system. The structures were solved by *direct methods (rac-2,4)* or *charge flipping (meso-2)*. Non-hydrogen atoms were refined with *anisotropic displacement parameters*. Hydrogen atoms were inserted at calculated positions and refined with riding model. C-H bond lengths in the aromatic and olefin bond systems were constrained at 0.950 Å, aliphatic CH₂ groups at 0.990 Å, and aliphatic CH₃ groups at 0.980 Å. The default values of SHELXL [11] were used for the riding-atom model. Fixed U_{iso} values of 1.2 times were used for all C(H) and C(H,H) groups, and fixed U_{iso} values of 1.5 times were used for all C(H,H,H) and O(H) groups.

The following software was used: Bruker SAINT software package [12] using a narrow-frame algorithm for frame integration; SADABS [13] for absorption correction; OLEX2 [14] for structure solution, refinement, molecular diagrams, and graphical user-interface; Shelxle [15] for refinement and graphical user-interface; SHELXS-2015 [11,16] for structure solution; SHELXL-2015 [11,17,18] for refinement; and Platon [19] for symmetry check. Crystal structure data is summarized in Table 1. For additional experimental parameters, see Table S1 in the Supplementary Materials.

Table 1. Crystal structure data of *rac-2*, *meso-2* and **4**.

	<i>Rac-2</i>	<i>Meso-2</i>	4
M (g/mol)	1012.72	718.70	631.77
Space group	P-1	C2/c	P-1
a (Å)	15.9737 (13)	30.408 (2)	11.5087 (4)
b (Å)	17.9202 (13)	14.8246 (12)	11.5335 (4)
c (Å)	18.7489 (19)	16.0429 (11)	13.5262 (5)
α (°)	117.544 (2)	90	75.6052 (14)
β (°)	93.715 (4)	103.653 (2)	76.2673 (14)
γ (°)	108.646 (2)	90	77.4586 (15)
V (Å ³)	4362.0 (7)	7027.6 (9)	1665.30 (10)
Z	4	8	2
R _{int}	0.073	0.064	0.036
R1 (I > 2 σ (I))	0.057	0.055	0.044
wR2 (all data)	0.191	0.151	0.119

3. Results and Discussion

3.1. Preparation of the Spiro Compounds

The unsubstituted parent compound was conveniently obtained by heating enantiomerically pure 2,2'-bis(bromomethyl)-1,1'-binaphthyl (*S*)_{ax}-1 in toluene with aqueous ammonia at 80 °C for 24 h in an autoclave. After removal of solvent and thoroughly washing of the white crystalline precipitate with water (*S,S*)_{ax}-2 was obtained in 94% yield. To the best of our knowledge, this simple “ammonia-route” was so far only used in a few cases [20,21]. Applying the same procedure to *rac-1* afforded a mixture of diastereomers as expected. ¹H-NMR showed the presence of *rac-2*/*meso-2* in a ratio of 55:45.

A more pronounced preference for the formation of either diastereomer by varying reaction conditions failed. Acetone was not suitable because of self-condensation, even under mild reaction conditions. More appropriate seemed acetonitrile, but the reaction was slower, and up to 27% of dinaphthoazepine **3** was detected (NMR). DMF yielded a complex mixture. Additionally, the addition of phase transfer catalysts or Et₃N did not alter the diastereomeric composition. Finally, temperatures between 80 and 100 °C, with efficient stirring in a two-phase system aqueous ammonia (25% *v/v*)/toluene were found to give the best results with the preferred formation of the *rac*-isomer. A preparative separation by chromatography was unsuccessful, but fractional crystallisation from THF/MeOH worked well. The crystalline material consisted largely of less-soluble *meso-2* (84%), while *rac-2* was enriched in the mother liquor (>90%). A second crystallisation afforded diastereomerically pure *meso*- and *rac-2* in 28% and 37% yield, respectively (Supplementary Materials, Figures S2–S7). The combined mother liquors from the second crystallisation could be recycled.

Alternatively, *meso-2* was obtained from (*S*)_{ax}-1 and (*R*)_{ax}-3 in quantitative yield.

3.2. Comparison of Solid-State Structures of *meso-2* and *rac-2* (Racemic and Enantiomeric)

Ready crystallisation of both diastereomers allowed the determination of the solid-state structure. *Rac-2* with D₂ symmetry crystallised in a non-chiral space group (P-1, Figure 3) differently from (*S,S*)_{ax}-2 (I 2₁ 2₁ 2₁; [3]), while *meso-2* revealed a nearly perfect S₄ symmetry in the solid state (Figure 4), a point group rarely found in organic molecules [22–28]).

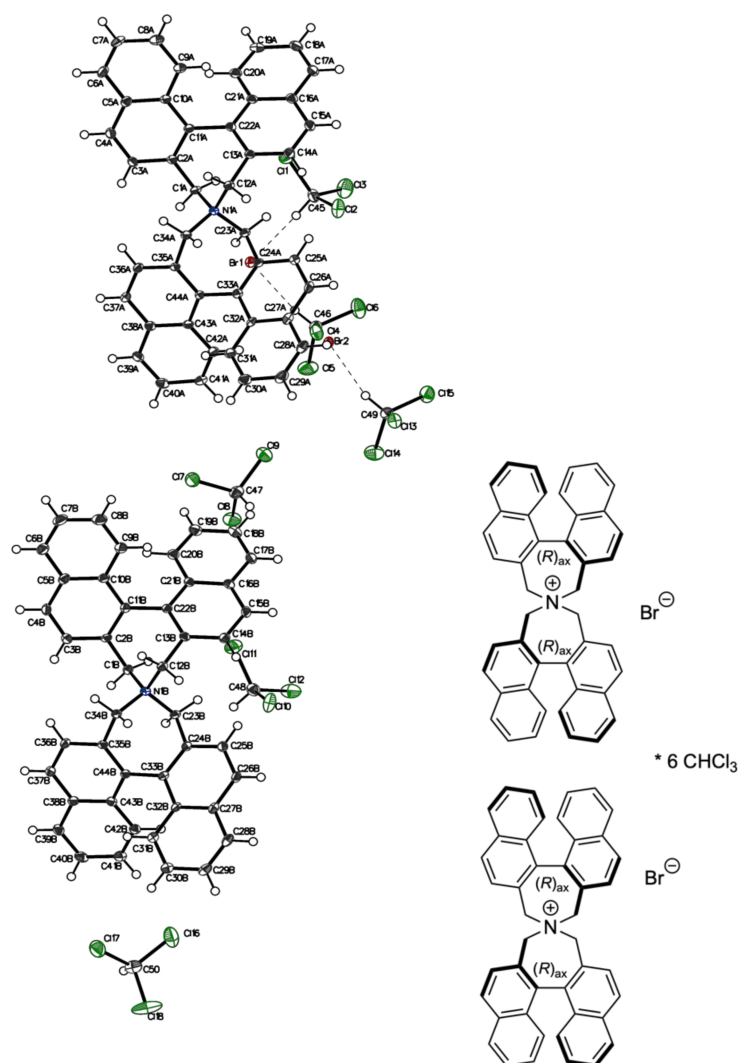


Figure 3. Displacement ellipsoid plot (**Left**) and chemical structure (**Right**) of *rac-2*. Ellipsoids were drawn at the 50% probability level. The two molecules are independent, and their conformations are the same, related by 1/2 translation in the *c*-axis direction. While both molecules shown in the asymmetric unit have the same (*R,R*)_{ax} configuration, the inversion centre produces two molecules of (*S,S*)_{ax} configuration, rendering the overall composition of the crystal racemic.

A more detailed inspection of structures showed significant deviations from ideal geometry, clearly visible when comparing the two azepinium units in each structure with different binaphthyl torsion angles (Table 2, Figure 5). Contrary to expectations, the structural peculiarities of diastereomers are less clearly evident. We find larger differences between the X-ray structures of *rac-2* and *enantiopure 2* (ref. [3]) than between *rac-2* and *meso-2*. These differences obviously arise from packing effects.

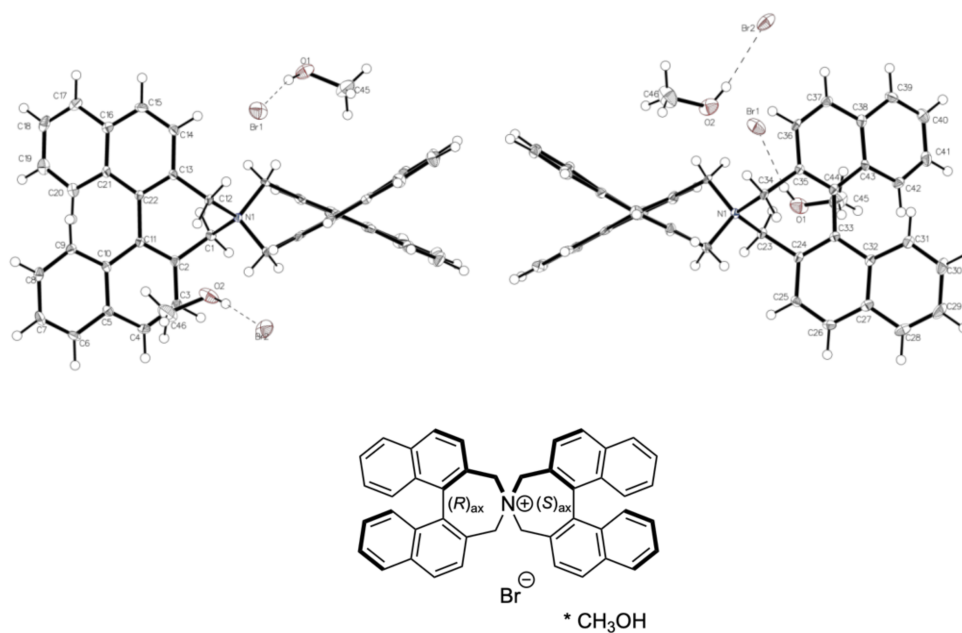


Figure 4. Displacement ellipsoid plot (top) and chemical structure (bottom) of *meso*-2. The molecular structure is plotted twice to fully present each binaphthyl system. While the plot features two bromide counterions, their occupancy is 1/2; hence, the proper count of one counter atom is preserved.

Table 2. Crystal structure parameters of *meso*- and *rac*-2 (the structure of the mirror image (*S,S*)_{ax}-2 was determined; CCDC code: GACVEM [3]) as well as (*R,R*)_{ax}-2 and selected torsion angles, bond angles, and distances.

	(<i>R,S</i>) _{ax} -2 (<i>meso</i>)	(<i>R,R</i>) _{ax} -2 [3]	(<i>R,R</i>) _{ax} / <i>(S,S</i>) _{ax} -2 (<i>rac</i>)
Torsion angle C2-C11-C22-C13 [°]	51.7(4)	50.7	50.6(5)
Torsion angle C24-C33-C44-C35 [°]	48.9(4)	55.5	49.0(5)
Bond angle C1-N1-C12 [°]	109.8(2)	111.3	110.9(3)
Bond angle C23-N1-C34 [°]	109.4(2)	109.9	110.6(3)
Bond angle C1-N1-C34 [°]	109.5(2)	108.9	112.1(3)
Bond angle C12-N1-C23 [°]	109.0(2)	108.9	112.2(3)
Bond angle C2-C1-N1 [°]	112.0(3)	110.4	113.8(3)
Bond angle C13-C12-N1 [°]	112.1(3)	110.4	112.6(3)
Bond angle C24-C23-N1 [°]	111.7(3)	110.9	113.5(3)
Bond angle C35-C34-N1 [°]	111.6(3)	110.9	112.9(3)
Distance C1-N1 [Å]	1.536(4)	1.522	1.525(3)
Distance C12-N1 [Å]	1.534(5)	1.522	1.531(4)
Distance C23-N1 [Å]	1.531(4)	1.540	1.526(5)
Distance C34-N1 [Å]	1.527(4)	1.540	1.521(5)

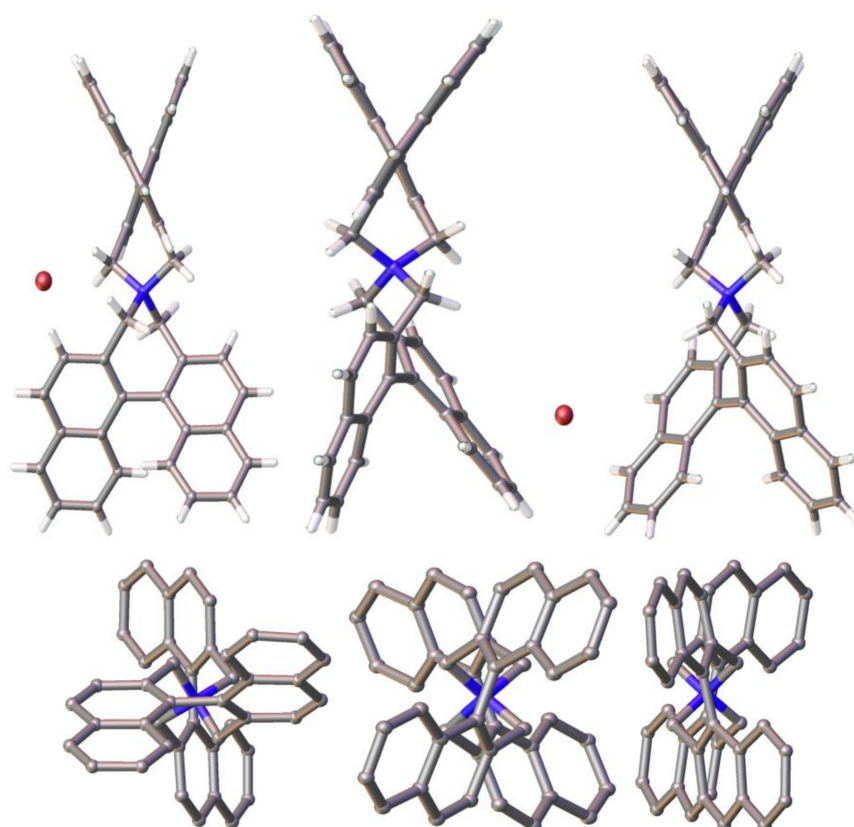


Figure 5. Crystal structures of $(R,S)_{ax}$ -2 (Left Side), $(R,R)_{ax}$ -2 (mirror image from GACVEM, [3] Middle), and $(S,S)_{ax}/(R,R)_{ax}$ -2 (Right Side). (Hydrogen atoms and solvent molecules omitted for clarity.)

3.3. Attempted Separation of Enantiomers of 2

Chromatographic separation on an analytical scale allowed the simultaneous determination of enantio- and diastereomeric composition of the crude mixture of spiro-ammonium bromides using a Chiralcel-ODH column, but separation factors were too small to run separations on a preparative scale ($\alpha = 1.7$). Fractionated crystallisation experiments with chiral counter anions remained unsuccessful.

3.4. Stevens Rearrangement of 2

Having synthesised compounds *rac*-2 and *meso*-2 of relatively high symmetry, we were interested in possible subsequent syntheses. The high symmetry of the molecules and thus the chemical equivalency of the reactive sites prospects a limited number of possible isomeric products. The reactivity of dibenzo- and dinaphthoazepinium compounds was investigated in the past (Figure 6). With good nucleophiles, ring opening was observed [29], while treatment with strong bases (KO^tBu , PhLi) resulted in a Stevens rearrangement with ring contraction [30]. Merely, for tetrabenzobisazepinium bromide, ring enlargement took place [31]. Additionally, non-racemic products were formed in the presence of chiral counter anions [32–34].

With tetranaphtho analogues 2, a similar behaviour was assumed, but as a consequence of rigidity of the structure, high regio- and stereocontrol of the rearrangement step was expected. Both *meso*- and *rac*-2 in THF were stirred with two equivalents of KO^tBu at r.t. overnight. NMR of the crude mixture revealed three (main) products derived from *meso*-2 but only one from *rac*-2 (Figure 7). All of these products are of the lowest molecular symmetry (C_1).

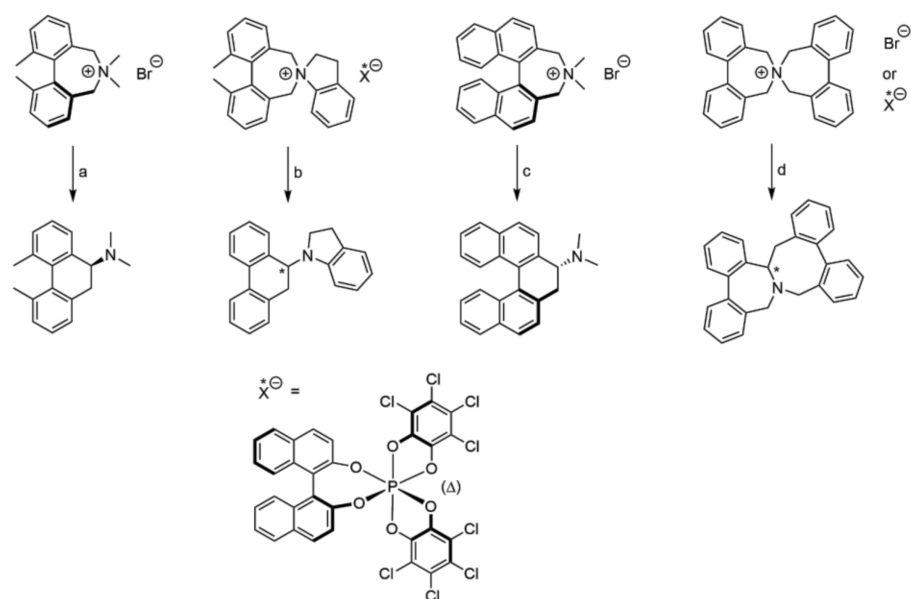


Figure 6. Stevens rearrangement of benzo and naphtho-annulated azepinium compounds. a: PhLi, Et₂O, [30] b: phosphazene base (X^- = Bis(tetrachlorobenzenediolato)mono([1,1']binaphthalenyl-2,2'-diolato)phosphate(V) anion) [32–34] c: KO^tBu, THF, [30] d: Ag₂O/MeOH, 180–190 °C (Br⁻; [31]), phosphazene base (X^- = Bis(tetrachlorobenzenediolato)mono([1,1']binaphthalenyl-2,2'-diolato)phosphate(V) anion) [32–34]).

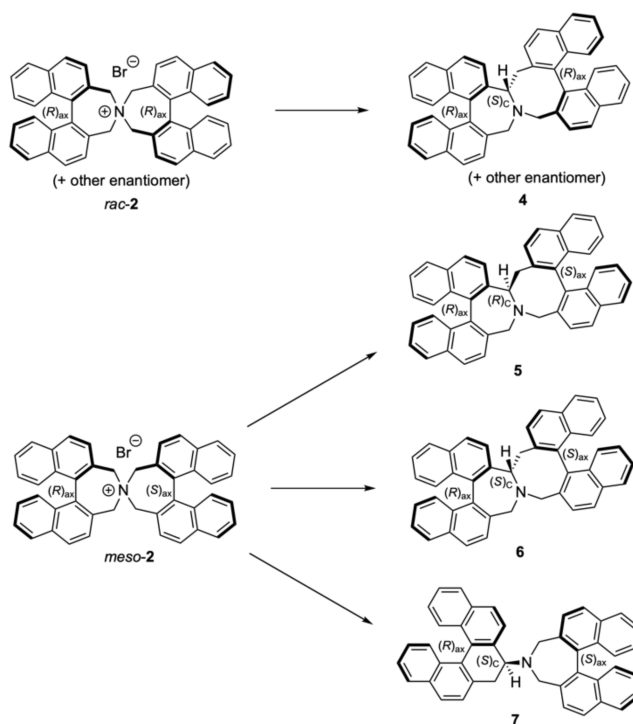


Figure 7. Stevens Rearrangement of *meso*- and *rac*-2. Conditions: THF or DCM, KO^tBu (2 equivalent) r.t., 10 h. Relative configuration of products: (*S*)_C(*R,R*)_{ax}-4, (*R*)_C(*R,S*)_{ax}-5, (*S*)_C(*R,S*)_{ax}-6, (*S*)_C(*S,S*)_{ax}-7.

After chromatographic purification, the rearranged product from *rac*-2 crystallised from DCM/acetone thus confirmed structure **4** for the tertiary amine with relative (*S*)_C(*R,R*)_{ax} configuration (Figure 8). Under optimised conditions (DCM, two equivalents of KO^tBu at r.t. overnight), **4** was isolated in 85% yield (Supplementary Materials, Figures S8 and S9). Rearranged products from *meso*-2 formed under similar conditions could only be partly separated. The ring contracted product **7** was isolated in 16% yield, while two iso-

mers **5** and **6** (70:30) were obtained in 64% yield as a mixture (Supplementary Materials, Figures S10–S13).

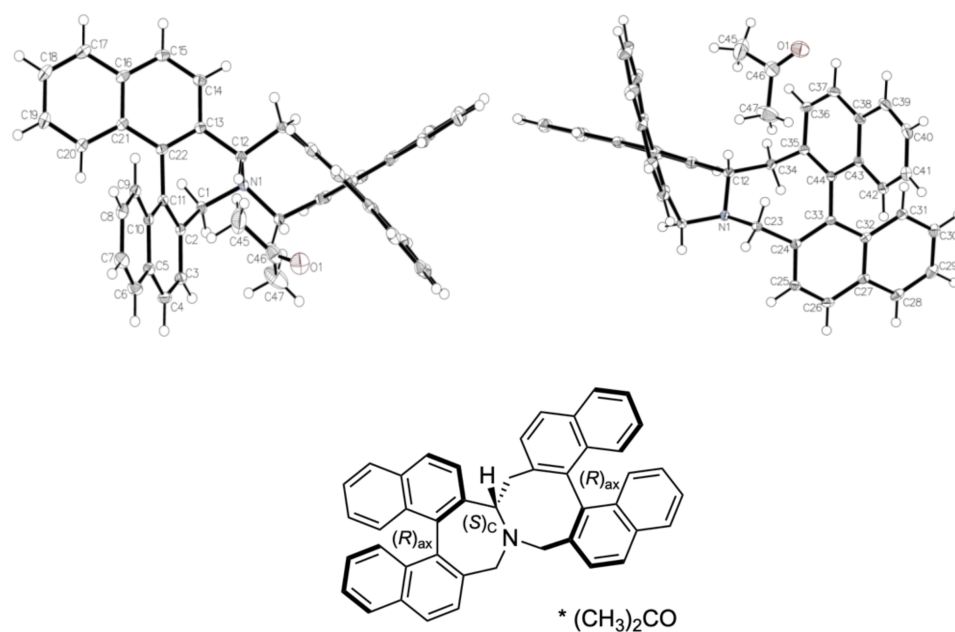


Figure 8. Displacement ellipsoid plot (**top**) and chemical structure (**bottom**) of Stevens rearrangement product **4**.

Further variations of conditions (*n*-BuLi, CH₃ONa, NaH, DBU, equivalents of base, temperature, reaction time) afforded slower conversion or decomposition. In the case of *meso-2*, the selectivity could not be improved. Methylation of **4** yielded the ammonium salt quantitatively (Supplementary Materials, Figures S14 and S15). Subsequent treatment with KO^tBu/THF at r.t. did not give any conversion. Applying more stringent conditions (*n*-BuLi in THF at r.t.) resulted in an inseparable mixture of products.

3.5. Intermolecular Structural Features

The crystal packing of the three crystal structures recorded is shown in Figure 9. Both *rac-2* (*Z* = 4) and **4** (*Z* = 2) are of *P*-1 symmetry and organised into sheets parallel to (110). The packing of *meso-2* (*Z* = 8) is more complex due to its higher *C* 2/*c* symmetry.

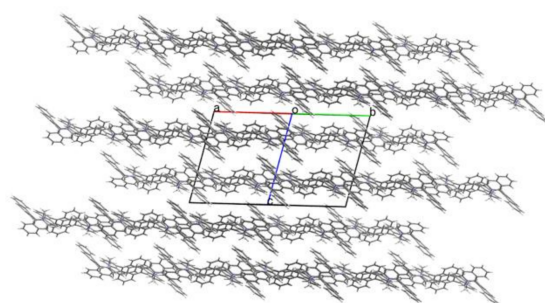


Figure 9. Cont.

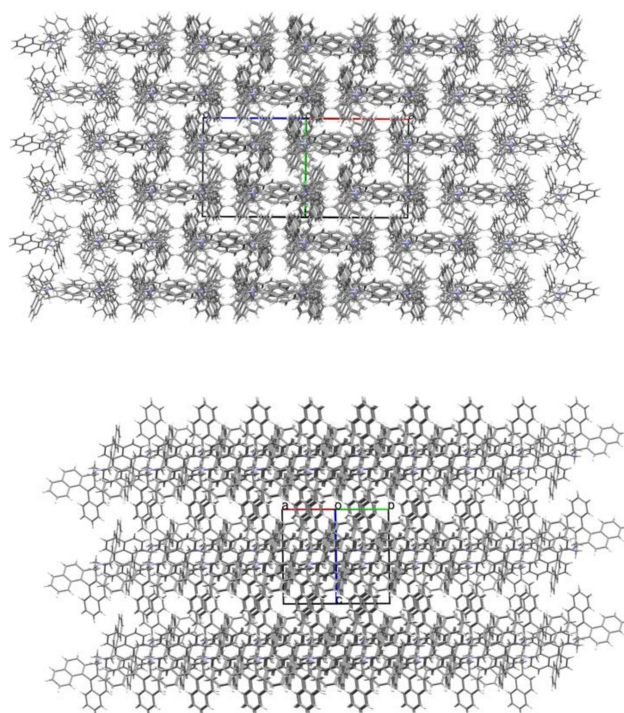


Figure 9. Crystal packing of *rac*-2 (top), *meso*-2 (middle) and 4 (bottom).

From those three crystal structures, only the crystal packing of *rac*-2 exhibits π - π interactions (Figure 10). In each case, the naphthyl planes of two opposite enantiomers overlap partially (Table S2 in the SI). Electrostatic interactions $\text{Cl}_3\text{CH}-\text{Br}^-$ reminiscent of hydrogen bridges were found between the counter ion and the co-crystallised solvents (Table S3 in the SI).

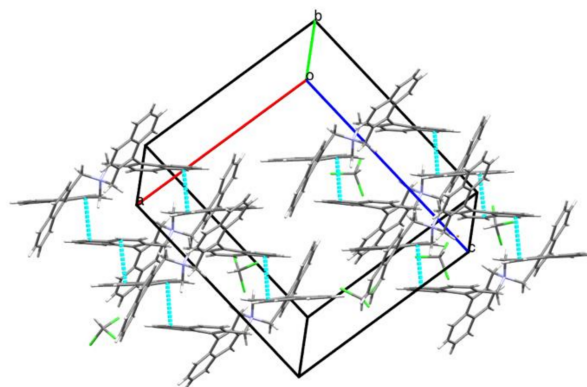


Figure 10. Crystal packing of *rac*-2. The blue lines mark close contacts between naphthyl planes of opposite enantiomers.

Cosolvent–anion hydrogen bridges were also found in the crystal structure of *meso*-2 between MeOH and Br^- (Table S3 in the SI). Additional close contacts were found between the positively polarised CH_2 groups adjacent to the quaternary nitrogen in *meso*-2 and both the Br^- counter ion ($d(\text{CH}_2-\text{Br}) = 2.764 \text{ \AA}$, 2.792 \AA) and the oxygen of MeOH ($d(\text{CH}_2-\text{O}) = 2.425 \text{ \AA}$, 2.498 \AA) (Figure 11).

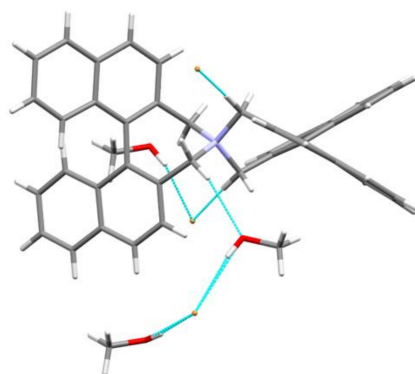


Figure 11. Close contacts between the CH₂ groups of *meso*-2, its counter ion Br[−], and solvent MeOH.

4. Conclusions

The spiro-compound 3,3',5,5'-Tetrahydro-4,4'-spirobi[dinaphtho[2,1-c:1',2'-e]azepin]-4-ium bromide **2** was synthesised from a racemic precursor and separated into two diastereomers by fractional crystallisation: (1) the racemic crystals of (*R,R*)_{ax}/*(S,S)*_{ax}-**2** and (2) the *meso* crystals of (*R,S*)_{ax}-**2**. While the former is a low-symmetry crystal structure (P-1) analogue of a known enantiopure crystal structure (I 2₁ 2₁ 2₁ [3]), the latter possesses a near-perfect S₄ improper rotation axis and belongs to point group S₄. This type of molecular symmetry is rare in organic chemistry and may be of interest in engineering molecules of high symmetry.

Of these crystal structures, only *rac*-**2** exhibits π-π interactions. In both crystal structures, the co-crystallised solvents (MeOH and CHCl₃) interact with the Br[−] counterions.

Both diastereomers undergo Stevens rearrangement when treated with ^tBuOK. While *meso*-**2** produced a mixture difficult to separate, the rearrangement of *rac*-**2** occurred diastereoselectively and yielded the ring-expansion product (S)_C(*R,R*)_{ax}/*(R)*_C(*S,S*)_{ax}-**4**.

Supplementary Materials: The following are available online at <https://www.mdpi.com/article/10.3390/sym13081365/s1>, Figure S1: HPLC Separation of Stereoisomers of **2**^{*}, Figure S2: (*R,S*)_{ax}-**2** (¹H NMR in CDCl₃), Figure S3: (*R,S*)_{ax}-**2** (¹H NMR in CD₂Cl₂), Figure S4: (*R,S*)_{ax}-**2** (¹³C NMR in CD₂Cl₂), Figure S5: (*R,R*)_{ax}/*(S,S)*_{ax}-**2** (¹H NMR in CDCl₃), Figure S6: (*R,R*)_{ax}/*(S,S)*_{ax}-**2** (¹H NMR in CD₂Cl₂), Figure S7: (*R,R*)_{ax}/*(S,S)*_{ax}-**2** (¹³C NMR in CD₂Cl₂), Figure S8: (*R,R*)_{ax}/*(S,S)*_{ax}-**4** (¹H NMR in CDCl₃), Figure S9: (*R,R*)_{ax}/*(S,S)*_{ax}-**4** (¹³C NMR in CDCl₃), Figure S10: mixture of **5** and **6** (70:30) (¹H NMR in CDCl₃), Figure S11: mixture of **5** and **6** (70:30) (¹H NMR in CDCl₃), Figure S12: **7** (¹H NMR in CDCl₃), Figure S13: **7** (¹³C NMR in CDCl₃), Figure S14: *N*-Methyl ammonium iodide of **4** (¹H NMR in CDCl₃), Figure S15: *N*-Methyl ammonium iodide of **4** (¹³C NMR in CDCl₃), Table S1: Experimental X-ray parameters and CCDC-Codes, Table S2: Short C-C contacts in *rac*-**2**, Table S3: Hydrogen bridges.

Author Contributions: Conceptualisation, literature search, resources, and synthesis, M.W.; X-ray measurement and refinement, A.P.-R. and N.G.; data curation, interpretation, visualisation, and writing of the manuscript, P.H. All authors have read and agreed to the published version of the manuscript.

Funding: This research received no external funding.

Institutional Review Board Statement: Not applicable.

Informed Consent Statement: Not applicable.

Data Availability Statement: Data is contained within the article and supplementary material.

Acknowledgments: Open Access Funding by the University of Vienna is gratefully acknowledged.

Conflicts of Interest: The authors declare no conflict of interest.

References

1. Shirakawa, S.; Maruoka, K. Recent Developments in Asymmetric Phase-Transfer Reactions. *Angew. Chem. Int. Ed.* **2013**, *52*, 4312–4348. [[CrossRef](#)] [[PubMed](#)]
2. Ooi, T.; Maruoka, K. Recent Advances in Asymmetric Phase-Transfer Catalysis. *Angew. Chem. Int. Ed.* **2007**, *46*, 4222–4266. [[CrossRef](#)] [[PubMed](#)]
3. Ooi, T.; Kameda, M.; Maruoka, K. Design of N-Spiro C₂-Symmetric Chiral Quaternary Ammonium Bromides as Novel Chiral Phase-Transfer Catalysts: Synthesis and Application to Practical Asymmetric Synthesis of α -Amino Acids. *J. Am. Chem. Soc.* **2003**, *125*, 5139–5151. [[CrossRef](#)] [[PubMed](#)]
4. Ooi, T.; Uematsu, Y.; Maruoka, K. New, Improved Procedure for the Synthesis of Structurally Diverse N-Spiro C₂-Symmetric Chiral Quaternary Ammonium Bromides. *J. Org. Chem.* **2003**, *68*, 4576–4578. [[CrossRef](#)]
5. Ooi, T.; Kameda, M.; Maruoka, K. Molecular Design of a C₂-Symmetric Chiral Phase-Transfer Catalyst for Practical Asymmetric Synthesis of α -Amino Acids. *J. Am. Chem. Soc.* **1999**, *121*, 6519–6520. [[CrossRef](#)]
6. Ooi, T.; Uematsu, Y.; Kameda, M.; Maruoka, K. Conformationally Flexible, Chiral Quaternary Ammonium Bromides for Asymmetric Phase-Transfer Catalysis. *Angew. Chem. Int. Ed.* **2002**, *41*, 1551–1554. [[CrossRef](#)]
7. Kitamura, M.; Shirakawa, S.; Maruoka, K. Powerful Chiral Phase-Transfer Catalysts for the Asymmetric Synthesis of α -Alkyl- and α,α -Dialkyl- α -amino Acids. *Angew. Chem. Int. Ed.* **2005**, *44*, 1549–1551. [[CrossRef](#)]
8. Ooi, T.; Takeuchi, M.; Kameda, M.; Maruoka, K. Practical Catalytic Enantioselective Synthesis of α,α -Dialkyl- α -amino Acids by Chiral Phase-Transfer Catalysis. *J. Am. Chem. Soc.* **2000**, *122*, 5228–5229. [[CrossRef](#)]
9. Hawkins, J.M.; Fu, G.C. Asymmetric Michael Reactions of 3, 5-Dihydro-4H-dinaphth [2, 1-c: 1', 2'-e] azepine with Methyl Crotonate. *J. Org. Chem.* **1986**, *51*, 2820–2822. [[CrossRef](#)]
10. Maigrot, N.; Mazeleyrat, J.P. New and Improved Synthesis of Optically Pure (R)- and (S)-2,2'-Dimethyl-1, 1'-binaphthyl and Related Compounds. *Synthesis* **1985**, *3*, 317–320. [[CrossRef](#)]
11. Sheldrick, G.M. A short history of SHELX. *Acta Cryst.* **2008**, *A64*, 112–122. [[CrossRef](#)]
12. Bruker SAINT, version 8.38B; Bruker AXS: Billerica, MA, USA, 2019.
13. Sheldrick, G.M. SADABS; University of Göttingen: Göttingen, Germany, 1996.
14. Dolomanov, O.V.; Bourhis, L.J.; Gildea, R.J.; Howard, J.A.K.; Puschmann, H. OLEX2. *J. Appl. Cryst.* **2009**, *42*, 339–341. [[CrossRef](#)]
15. Huebschle, C.B.; Sheldrick, G.M.; Dittrich, B. ShelXle: A Qt graphical user interface for SHELXL. *J. Appl. Cryst.* **2011**, *44*, 1281–1284. [[CrossRef](#)] [[PubMed](#)]
16. Sheldrick, G.M. SHELXS; University of Göttingen: Göttingen, Germany, 1996.
17. Sheldrick, G.M. SHELXL; University of Göttingen: Göttingen, Germany, 1996.
18. Sheldrick, G.M. Crystal structure refinement with SHELXL. *Acta Cryst.* **2015**, *C71*, 3–8. [[CrossRef](#)]
19. Spek, A.L. Structure validation in chemical crystallography. *Acta Cryst. D* **2009**, *65*, 148–155. [[CrossRef](#)] [[PubMed](#)]
20. Kano, T.; Lan, Q.; Wang, X.; Maruoka, K. Effects of Aromatic Substituents on Binaphthyl-Based Chiral Spiro-Type Ammonium Salts in Asymmetric Phase-Transfer Reactions. *Adv. Synth. Catal.* **2007**, *349*, 556–560. [[CrossRef](#)]
21. Hashimoto, T.; Tanaka, Y.; Maruoka, K. Symmetrical 4,4',6,6'-tetraarylbinaphthyl-substituted ammonium bromide as a new, chiral phase-transfer catalyst. *Tetrahedron Asym.* **2003**, *14*, 1599–1602. [[CrossRef](#)]
22. Sakamoto, Y.; Suzuki, T. Tetrabenzo[8]circulene: Aromatic Saddles from Negatively Curved Graphene. *J. Am. Chem. Soc.* **2013**, *135*, 14074–14077. [[CrossRef](#)]
23. Lutz, M.R.; Zeller, M.; Sarsah, S.R.S.; Filipowicz, A.; Wouters, H.; Becker, D.P. Synthesis, crystal structure and rearrangements of orthocyclophane cyclotetrameratrylene (CTTV) tetraketone. *Supramol. Chem.* **2012**, *24*, 803–809. [[CrossRef](#)]
24. Ahn, H.C.; Yun, S.; Choi, K. A proline-based macrocyclic amide with S₄ symmetry. *Chem. Lett.* **2008**, *37*, 10–11. [[CrossRef](#)]
25. Coles, S.J.; Davies, D.B.; Eaton, R.J.; Hursthouse, M.B.; Kilic, A.; Shaw, R.A.; Uslu, A. Stereogenic properties of spiranes combined with four equivalent conventional centers of chirality. *Dalton Trans.* **2007**, *20*, 2040–2047. [[CrossRef](#)]
26. Kozhushkov, S.I.; Kostikov, R.R.; Molchanov, A.P.; Boese, R.; Benet-Buchholz, J.; Schreiner, P.R.; Rinderspacher, C.; Ghiviriga, I.; De Meijere, A. Tetracyclopropylmethane: A unique hydrocarbon with S₄ symmetry. *Angew. Chem. Int. Ed.* **2001**, *40*, 180–183. [[CrossRef](#)]
27. Mislow, K. Nonactin and the coupe du roi. *Croatica Chem. Acta* **1985**, *58*, 353–358.
28. Murray-Rust, P.; Riddell, F.G. The Stability and Conformation of the 1,3,6,8-Tetraazatricyclo[4.4.1.13,8]dodecane System: The Structure of the Condensation Product of 1,2-Diaminocyclohexane and Formaldehyde. *Can. J. Chem.* **1975**, *53*, 1933–1935. [[CrossRef](#)]
29. Stará, I.G.; Starý, I.; Závada, J. Nucleophilic Cleavage of 4,5-Dihydro-3H-dinaphth[2,1-c:1',2'-e]azepinium Quaternary Salts. A Convenient Approach to New Axially Dissymmetric and Axially Asymmetric Ligands. *J. Org. Chem.* **1992**, *57*, 6966–6969. [[CrossRef](#)]
30. Stará, I.G.; Starý, I.; Tichý, M.; Závada, J.; Hanus, V. Stereochemical Dichotomy in the Stevens Rearrangement of Axially Twisted Dihydroazepinium and Dihydrothiepinium Salts. A Novel Enantioselective Synthesis of Pentahelicene. *J. Am. Chem. Soc.* **1994**, *116*, 5084–5088. [[CrossRef](#)]
31. Wittig, G.; König, G.; Clauss, K. 1,2,3,4,7,8,9,10-Tetrabenzo-cyclododecahexaen. *Liebigs Ann. Chem.* **1955**, *593*, 127. [[CrossRef](#)]
32. Vial, L.; Lacour, J. Conformational Preference and Configurational Control of Highly Symmetric Spiro[dibenzazepinium] Cation. *Org. Lett.* **2002**, *4*, 3939–3942. [[CrossRef](#)]

-
33. Vial, L.; Gonçalves, M.-H.; Morgantini, P.-Y.; Weber, J.; Bernardinelli, G.; Lacour, J. Unusual Regio- and Enantioselective [1,2]-Stevens Rearrangement of a Spirobi[dibenzazepinium] Cation. *Synlett* **2004**, *9*, 1565–1568. [[CrossRef](#)]
 34. Gonçalves-Farbos, M.-H.; Vial, L.; Lacour, J. Enantioselective [1,2]-Stevens rearrangement of quaternary ammonium salts. A mechanistic evaluation. *Chem. Commun.* **2008**, *7*, 829–831. [[CrossRef](#)]